FLOW IN POROUS MEDIA WITH SLIP BOUNDARY CONDITION

S. Berg, A. W. Cense, J. P. Hofman, R. M. M. Smits
Shell International Exploration and Production B.V.,
Kesslerpark 1, 2288 GS Rijswijk (Zh), The Netherlands

This paper was prepared for presentation at the International Symposium of the Society of Core Analysts held in Calgary, Canada, 10-12 September 2007

ABSTRACT

Endpoint relative permeabilities larger than one ($k_r > 1$) for 2-phase flow in porous rock samples have been reported several times in literature. This holds in particular when the non-wetting phase is the majority phase and the wetting phase is present only as thin wetting films covering the rock surface. Cases where $k_r > 1$ were debated over many years and there are reports in the literature indicating that often data is re-normalized such that $k_r \leq 1$ since it is often suspected as a measurement error. In this presentation we show that there is a real physical explanation for the effect of $k_r > 1$. We draw an analogy between this observation and a possible slip-boundary condition. For comparison, flow in capillary tubes with a slip boundary condition is considered where hydrodynamic flow properties can be calculated analytically. The flux of the non-wetting phase is in many cases about 2-4 times higher when a small-amount of the wetting phase is present which would be compatible with slip lengths in the range of 100-700 nm in sandstone reservoirs. For a fixed slip length the flux in capillary tubes is increasing for decreasing capillary radius. This dependency is qualitatively found in our data indicating that slip could indeed be a plausible explanation for the observation of $k_r > 1$. Thus we conclude that $k_r > 1$ is a real effect and should be accepted as such. No data should be re-normalized as it would not reflect the true flow properties of the rock.

1 INTRODUCTION

In the oil industry, special core analysis (SCAL) is an essential step in the work flow to determine the performance of an oil reservoir with respect to it's flow performance. In special core analysis, the (oil- or water-) saturation dependent parameters like the capillary pressure P_c and the relative permeabilities k_r [Dake (1978)] are determined. In particular the relative permeabilities of water and oil are important to predict how fast oil and water will flow in an oil reservoir and are therefore very critical parameters.

Fluid flow for a single phase through a porous medium can be described with Darcy's law $Q = A \cdot (K / \mu) \cdot \nabla p$ where Q is the flux, A is the cross sectional area, K is the (absolute) permeability of the medium for single phase flow and μ is the viscosity. For 2-phase flow (e.g. water *w* and oil *o*) Darcy's law is modified to

$$Q_w = \frac{A \cdot K_w}{\mu_w} \nabla p_w \qquad Q_o = \frac{A \cdot K_o}{\mu_o} \nabla p_o \tag{1}$$

with effective permabilities K_w and K_o. Introducing the concept of relative permeabilities $k_{r,w}$ and $k_{r,o}$ for water and oil we obtain $K_w = k_{r,w} \cdot K$ and $K_o = k_{r,o} \cdot K$. The relative permeabilities are dependent on the saturation of the phases S, i.e. $k_{r,w}=k_{r,w}(S_w)$ and $k_{r,o}=k_{r,o}(S_o)$. It is usually assumed that the relative permeabilities $0 \le k_r \le 1$. But there are several reports in the literature that explicitly show endpoint relative permeabilities $k_r>1$ [Dullien (1959), McPhee (1994), McPhee&Arthur (1994), Karabakal&Bagci (2004), Arps&Roberts (1955), Ehrlich (1993), Mikkelsen&Scheie (1991)]. By endpoint relative permeabilities we mean the water relative permeability $k_{r,w}$ at residual oil saturation $S_{o,r}$ and the oil relative permeability $k_{r,o}$ at connate water saturation $S_{w,c}$. In several examples in the literature [McPhee (1994), McPhee&Arthur (1994), Karabakal&Bagci (2004)] the (near) endpoint relative permeabilities $k_r>1$ in particular when the non-wetting phase is the majority phase and the wetting phase is present only as thin wetting films covering the rock surface. In other words, in the presence of very small amounts of a wetting phase the permeability of a non-wetting phase is actually larger than the absolute permeability of the rock.

In the literature, this effect does not usually appear since often the endpoint relative permeabilities are normalized to 1 [McPhee&Arthur (1994)]. But according to publications in the peer-reviewed literature, end point relative permeabilities are measured to be up to $1 \le k_r \le 2.4$ [ODEH (1959), McPhee (1994), McPhee&Arthur (1994)]. In Refs. [McPhee (1994)] and [Karabakal&Bagci (2004)] in particular the end point permeability for the non wetting phase $k_r>1$. In oil-wet systems (wetting-index -1) the $k_{r,w}(S_{w,c})>1$ and in water-wet systems $k_{r,o}(S_{o,r}) > 1$.

2 EXPERIMENTAL

The data shown in this publication has been collected over many years in Shell laboratories in SCAL studies on oil fields in different regions of the world. The data has been entered into a data base that contains a set of parameters on the samples, including porosity ϕ and absolute permeability K, but also the relative permeabilities k_r for oil and water as a function of the water saturation S_w. The standard procedure is for core plugs to be cleaned (Soxhlett hot extraction cleaning with toluene and chloroform/methanol azeotrope) and then "aged" to restore their reservoir properties. After cleaning, the state of the samples is referred to as "un-aged" and several parameters like the absolute permeability K_{brine} are measured. In general, sandstones in oil reservoirs show water-wet to intermediate-wet behaviour. Aged samples can be somewhat less water-wet than un-aged samples. Relative permeabilities have been measured using the steady state technique, the unsteady-state technique, and the centrifuge. In general, relative

permeabilities for water and oil are obtained from permeabilities that are measured according to Darcy's law for single phase flow. The relative permeabilities are obtained by normalizing the saturation-dependent permeabilities $K_o(S_w)$ and $K_w(S_w)$ with the brine single phase absolute permeability K.

2.1 Observations of k_r>1

For instance in a sandstone reservoir in New Zealand it was found that $k_{r,o}(S_{w,c})$ can reach values between 1.2 and 1.5. For a sandstone field in Oman the oil endpoint permeability K_o is a factor 1.2-2.9 larger than the brine permeability K_w. In order to give an overview over the distribution of relative permeabilities in Fig. 1 we plot water and oil end point relative permeabilities $k_{r,w}(S_{w,c})$ and $k_{r,o}(S_{o,r})$ as a function of the water saturation S_w for a set 130 individual measurements taken from 43 sandstone reservoirs.

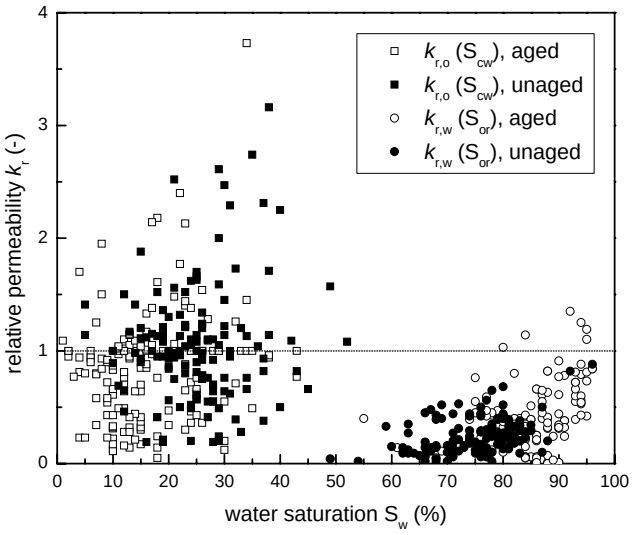

Fig. 1: Water and oil end point relative permeabilities in 43 sandstone reservoirs plotted as function of the water saturation S_w.

The data plotted in Fig. 1 bear large similarities with those shown by [McPhee (1994)]. Sandstone reservoirs are known to have a more water-wet tendency. Fig. 1 shows $k_{r,o} > 1$ in particular for un-aged and presumably even more water-wet samples. Some examples for $k_{r,w} > 1$ are found for the aged samples where presumably the rock has become more oil-wet due to the exposure to crude oil. So for the more water-wet case $k_{r,o} > 1$ and for the more oil-wet case $k_{r,w} > 1$.

In the literature the observation of $k_r > 1$ is often termed "lubricating effect" [McPhee&Arthur (1994), Karabakal&Bagci (2004), Dong et al. (2006)] but in most cases no further explanation about fundamental physical mechanisms is given. In [Ehrlich (1993)] the effect of $k_r > 1$ is discussed in the context of viscous coupling in porous media [Ayub&Bentsen (1999)] linking it to an effect of interfacial shear viscosity. Effectively oil-water interfaces can then act as slip boundaries [Deen (1998)].

In the following we investigate how an explicit formulation of a slip boundary condition at the oil-water interface can explain the observations of $k_r > 1$ in SCAL experiments.

3. SLIP BOUNDARY CONDITION

In fluid mechanics it is generally accepted that at an interface between two (mobile) fluids the tangential velocities *v* have to be continuous, i.e. $v_1 = v_2$ [Deen (1998)] (no-slip boundary condition). In the past it was also assumed that the boundary condition for fluid flow past a solid wall is a no-slip boundary condition as well [Deen (1998)], i.e. when a fluid flows past a solid substrate which is at rest the tangential velocity at the wall vanishes, $v(r=R)=0$. During the past years, various experiments showed a non-vanishing tangential velocity, the so-called slip velocity v_{slip} [ZHU&GRANICK (2001), ZHU&GRANICK (2002)]. In Fig. 2 A and B the velocity profiles for pipe flow is sketched with a no-slip boundary condition and on the right with a slip boundary condition.

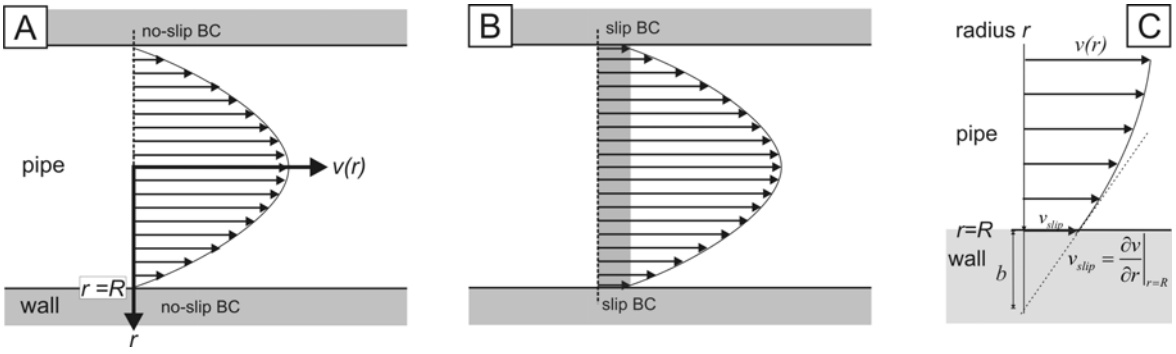

Fig. 2: Pipe flow with no-slip (A) and slip (B) boundary conditions. For slip the tangential velocity of the fluid at the wall is $v_{slip} > 0$. The slip velocity right at the wall v_{slip} can be derived from the slip length *b* which is defined via extrapolation of the velocity gradient into the wall (C).

The slip velocity can be parameterized in the so-called Navier slip boundary condition [Navier (1827), Brochard&deGennes (1992), Vinogradova (1995), deGennes (2002), deGennes (1985)]

$$v_{slip} = b \cdot \left. \frac{\partial v(r)}{\partial r} \right|_{r=R} \tag{2}$$

where the slip length b is constructed via linear extrapolation into the wall to the hypothetical location where v=0. For the extrapolation, the velocity gradient $\partial v / \partial r$ at the wall (r=R) is used. The geometrical construction is sketched in Fig. 2C.

Slippage is observed in various systems at liquid-solid interfaces and can strongly influence hydrodynamic behavior in microscale and nanoscale flows. Contributing factors include poor interfacial wettability or weak molecular attraction between phases [Tolstoi (1952), Blake (1990)], surface roughness [Miksis&Davis (1994)], high shear rates [Thompson&Troian (1997)], a reduction in polymer interfacial viscosity [Brochard ET AL. (1990)], and nucleation of nanobubbles at hydrophobic surfaces [Vinogradova ET AL. (1995)]. Despite the enormous interest in slip behavior, there is yet no consensus on which parameters control the degree of slip in simple fluids [Priezjev&Troian (2004)]. In this publication, the relevance of slip for oil recovery and special core analysis (SCAL) is addressed.

3.1 Experimentally Observed Slip Lengths

During the past years slip has been experimentally observed in several studies in two classes of systems. One class involves polymer melts [Priezjev&Troian (2004), Priezjev&Troian (2006)] and will not be discussed any further in this work. The second class is focusing on the flow of simple liquids and water past substrates. Most studies employ model systems with well-defined geometries and solid-liquid interfaces with a roughness of less than 1 nm. Experimental parameters like the substrate wettability, the fluids [Zhu&Granick (2001)], the shear rates and surface roughness [Zhu&Granick (2002)] are varied systematically. Slip is studied in capillaries in pressure-driven flow [Schnell (1956), Chuarev ET AL. (1984), Watanabe ET AL. (1999)], in squeeze-flow geometries with a surface-force apparatus [Horn ET AL. (2000), Zhu&Granick (2001), Zhu&Granick (2002)] and using particle image velocimetry (PIV) [Tretheway&Meinhart (2002)]. In most cases an apparent slip boundary condition is observed with slip lengths b ranging from nanometers (20 nm [Cottin-Bizonne ET AL. (2005)], 30 nm [Choi ET AL. (2003)], 30-70 nm [Chuarev ET AL. (1984)], 30 - 50 nm [Horn ET AL. (2000)]) to the micrometer range (0-2 μm [Zhu&Granick (2001)], 1 μm [Tretheway&Meinhart (2002)], 0-2 μm [Zhu&Granick (2001)], 1-10 μm [Schnell (1956)], 20-50 μm [Choi&Kim (2006)], 100 μm [Watanabe ET AL. (1999)], 0.1-300 μm [Migler ET AL. (1993)]). One common observation, for example in the case of slip in water flowing past hydrophobic interfaces, is that slip is found in systems where the fluid is not wetting the interface [Choi&Kim (2006)]. The situation that would mimic our scenario in terms of geometric dimensions most closely (except for the wettability) is the observation that a hydrophobic coating of 2.3 nm thickness (monolayer) in 30 μm x 300 μm wide micro channels can produce slip lengths of 1 μm [Tretheway&Meinhart (2002)].

3.2 Microscopic Origins of Slip

The microscopic origin of slip depends most likely on the system considered. For instance slip in polymeric systems may be caused by completely different mechanisms than slip in systems where wetting behavior plays a major role. But even there the

microscopic origin is still under heavy debate. For instance in the system of water flowing past a hydrophobic surface where slip has been experimentally observed it is argued if the fluid actually flows past a ”carpet” of nano-bubbles covering the hydrophobic surface. There are some experimental observations of such nano-bubbles with the atomic force microscope (AFM) [Zhu&Granick (2001), Tyrrell&Attard (2001), Zhu&Granick (2002)]. It is however under scientific debate if these nanobubbles were there in the first place [Lauga&Stone (2003)] or nucleated during the measurement itself. In neutron scattering experiments [Doshi ET AL. (2005)] it was actually found that close to a hydrophobic interface water has a different structure and a lower density and also reduced viscosity which could explain the apparent slip behavior. Using x-ray scattering a recent study found that there is a small “gap” between water and a hydrophobic substrate [Mezger ET AL. (2006)].

In the case where the fluid structure near a wall can be described by a two layer system where a bulk fluid (viscosity μ_{bulk}) is flowing past a solid wall and a microscopic layer (thickness δ) close to the wall exhibits a lower viscosity $\mu_{wall} < \mu_{bulk}$, the slip boundary condition can be modeled via the construction displayed in Ref. [Vinogradova (1995)] obtaining the relationship [Choi&Kim (2006)] $b = \delta \cdot \left(\mu_{bulk} / \mu_{wall} - 1 \right)$. Applying this relation to the experimental situation for water on hydrophobic surfaces with $\delta \sim 0.5$ nm typically and the known viscosity ratio $\mu_{bulk} / \mu_{wall} \sim 50$ a slip length b = 25 nm is obtained [Doshi ET AL. (2005)] which is well within the range reported in the literature.

3.3 Pipe Flow with Wall Slip

The velocity profile for pressure-driven flow in a pipe is sketched in Fig. 2A. The typical parabolic Poiseuille velocity profile results from a no-slip boundary condition with a vanishing tangential velocity at the wall. For a slip boundary condition the velocity right at the wall is finite as shown in Fig. 2 B and C. In order to derive the explicit form of the velocity profile $v(r)$ and the flux Q for pipe flow we start out with the Navier-Stokes equation [Deen (1998)] which describes the momentum transport in a Newtonian fluid with viscosity μ and density ρ. To describe the flow in a pipe a cylindrical coordinate system (r,θ,z) is chosen. For steady, fully developed flow $v=v(r)$ and $\partial v/\partial t=0$. In the absence of inertial components in the z-direction, $(\mathbf{v} \cdot \nabla \mathbf{v})_z = \mathbf{0}$. In the absence of pressure gradients in the r and θ directions, only $\partial p/\partial z \neq 0$ leading to $p=p(z)$. Using the Laplace operator in cylindrical coordinates [Deen (1998)] we obtain for the flow equation

$$0 = -\frac{\partial p}{\partial z} + \mu \frac{1}{r} \frac{\partial}{\partial r} \left(r \frac{\partial v_z}{\partial r} \right) \tag{3}$$

Rearrangement and integration over r results in

$$\frac{\partial v_z}{\partial r} = \frac{1}{\mu} \frac{\partial p}{\partial z} \frac{r}{2} + C_1 \tag{4}$$

Symmetry at the center of the pipe (r=0) requires $\partial v / \partial r\big|_{r=0} = 0$ is the first boundary condition (BC1). It follows that C_1=0. Further integration results in

$$v_z(r) = \frac{1}{\mu}\frac{\partial p}{\partial z}\frac{r^2}{4} + C_2 \tag{5}$$

with the constant of integration C_2 being determined by the boundary condition at the wall r=R (BC2). Inserting the slip boundary condition from eq. 2 in eq. 5 at r=R and using eq. 4 at r=R allows the determination of C_2 resulting in the velocity profile $v_z(r)$ [Tretheway&Meinhart (2002)]

$$v_z(r) = -\frac{1}{\mu}\frac{R^2}{4}\frac{\partial p}{\partial z}\left(1 - \frac{r^2}{R^2} + \frac{2b}{R}\right) \tag{6}$$

The flux Q is obtained by integrating $v_z(r)$ from eq. 6 over the pipe cross section [Lauga&Stone (2003)]

$$Q = \int_0^R 2\pi r v_z(r) dr = -\frac{\pi R^4}{8\mu}\frac{\partial p}{\partial z}\left(1 + \frac{4b}{R}\right) \tag{7}$$

Practically, this means that in the presence of slip at the same pressure a larger amount of fluid is transported through the pipe per unit time. In Fig. 3 the flux ratio for slip / no slip *Q(R,b)/Q(R,b=0)* is displayed as function of the pipe radius R for three different slip lengths in the range b=20-100 nm. This is a reasonable range for water flowing past a hydrophobic interface.

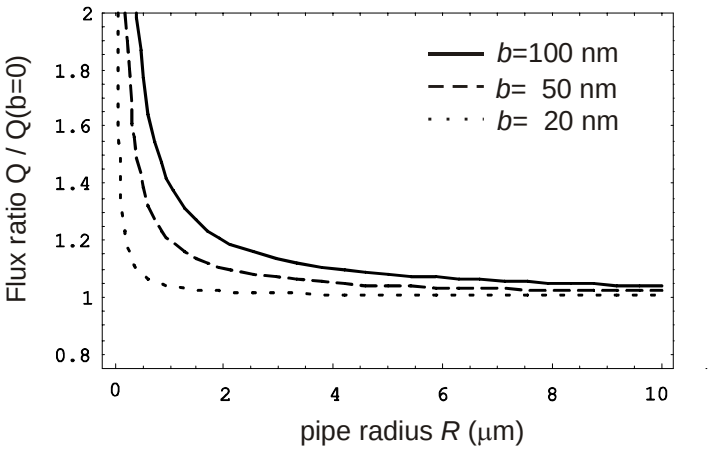

Fig. 3: Flux ratio $Q(b)/Q(b=0)$ for different slip lengths b as function of pipe radius R.

For b=0 the classical Poiseuille flux with $Q \propto \mu R^4$ is obtained [Deen (1998)]. The first order correction term *1 + 4 b/R* due to slip can be obtained by imagining that the pipe radius *R* is increased by the slip length *b* to *R+b*.

4. DISCUSSION

Most experimental observations in the literature and in our data very consistently show that $k_r>1$ for the non-wetting phase at saturations where the wetting phase is reduced to very thin and presumably immobile films covering the rock surface. Potentially these wetting films are reduced to layers of only a few nanometers thickness that are in the end responsible for the wettability alteration of the rock [Lord&Buckley (2002)]. Apparently the thin wetting films act as "lubricant" for the non-wetting phase [McPhee (1994)]. But so far it is an open question what the microscopic mechanism for the "lubrication" is.

Single phase flows in a tube and in a porous medium bear large similarities. In order to describe basic properties like permeability, equivalent capillary tube models are employed [Dullien (1959)]. The structures of Darcy's law and Poiseuille flux (eq. 7) are very similar (flux due to pressure driven flow) as well. Single- and two-phase flow in a porous medium is often described in so-called pore-networks [Hui&Blunt (2000)] where pore bodies are connected via tubes in which the fluid flows. Therefore, an analogy between the flow in porous media and flow in capillary tubes is used to draw the analogy between the observation of $k_r>1$ and a slip boundary condition for the endpoints.

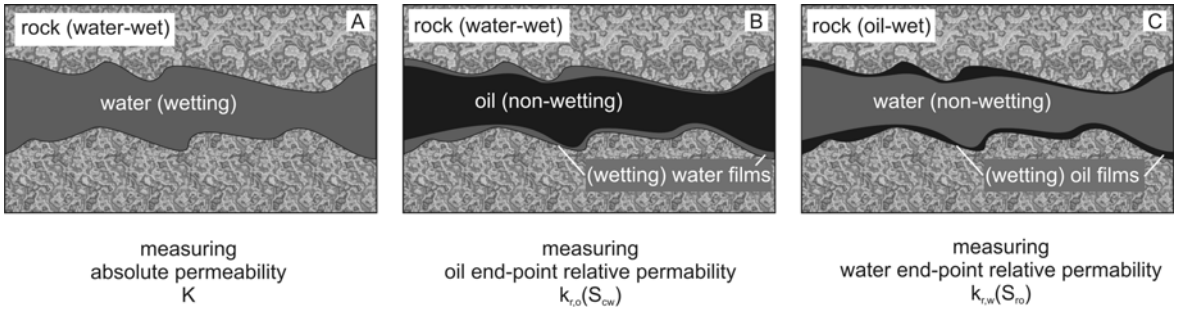

Fig. 4: Fluid configurations for single phase flow (A) and two phase flow with water-wet rock (B) and oil-wet rock (C) where the non-wetting phase is flowing past immobile wetting layers.

Honoring this analogy, the flow geometry and phase distribution is sketched in Fig. 4. The (immobile) film of the wetting phase covering the rock surface may produce an effective slip boundary condition for the flow of the non-wetting fluid resulting in an additional flux contribution similar to that in eq. 7. The ratio of the flux with slip Q and without slip $Q_0 = Q(b=0)$ computes to

$$\frac{Q}{Q_0} = \frac{Q(b,R)}{Q(b=0,R)} = 1 + \frac{4b}{R} \qquad (8)$$

This quantity is similar to the endpoint relative permeability k_r of the non-wetting phase. The flux Q_0 is measured in single phase flow according to Darcy's law as $Q_0 = Q(b=0,R) = K_{abs} \cdot A / \mu_o \nabla p_o$. The oil flux $Q = Q(S_{w,c})$ at the irreducible water saturation is measured in 2-phase flow as $Q(b,R) = K_o(S_{w,c}) \cdot A / \mu_o \nabla p_o$. Thus the ratio $Q / Q_o = K_o(S_{w,c}) / K_{abs} = k_{r,o}(S_{w,c})$. With eq. 8 we obtain $k_{r,o}(S_{w,c}) = 1 + 4b / R$.

In this analogy the wetting layers are assumed to homogeneously cover the rock surface as immobile layers with uniform thickness of only a few nanometers. More complicated configurations are not considered. Such films could have been formed by adsorption of naphthenic acids or asphaltenes [Lord&Buckley (2002)] that are both known to change the wettability to oil-wetness. Since they are only from molecular thickness to a few nanometers thickness [Lord&Buckley (2002)] they do not reduce the cross section of the few micrometer thick flow channels in any significant way.

Eq. 8 is displayed in Fig. 3. It demonstrates that for a typical effective pore radius in the micrometer range and slip lengths of about 100 nm, $k_{r,o}(S_{w,c})$ can take values similar to the examples of $k_r > 1$ reported in literature [McPhee (1994)].

From this comparison, slip is a plausible explanation for endpoint relative permeabilities larger than one. A more direct comparison with the theoretical model (eq. 8) is not possible as data on effective pore diameters are missing. But for the data in Fig. 1 taken from a Shell "relperm database" such a comparison is possible. An equivalent capillary radius r_e for a pseudo-3D capillary model of the porous network can be estimated [Dullien (1959)] as $r_e \approx 5 \cdot \sqrt{K / \phi}$ where K is the absolute permeability and ϕ is the porosity.

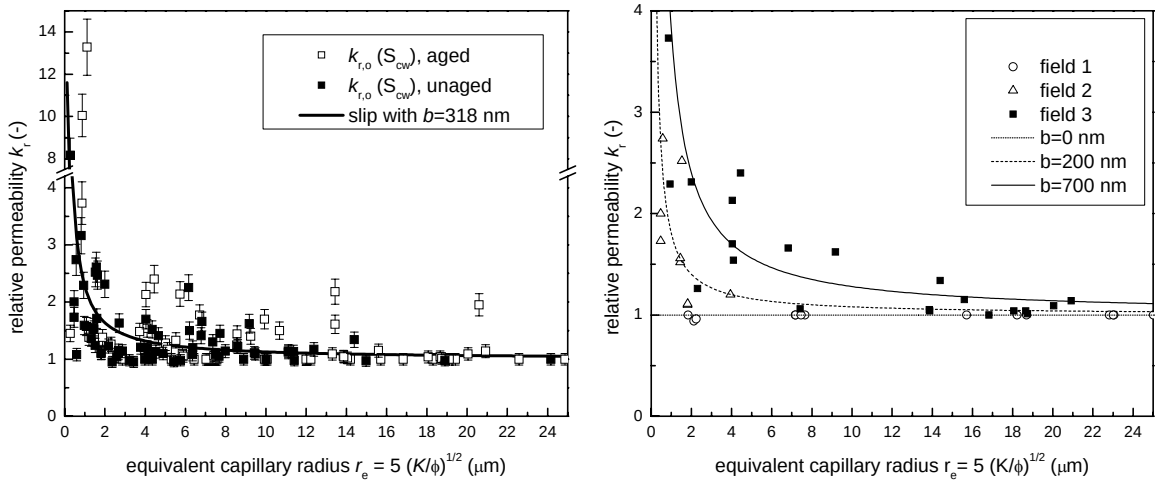

Fig. 5: On the left oil end point relative permeabilities $k_{r,o}(S_{cw})$ from Fig. 1 are plotted as a function of an effective capillary radius $r_e \approx 5 \cdot \sqrt{K/\phi}$. Data with $k_{r,o}(S_{cw})$>0.95 for aged and un-aged samples from Fig. 1. The solid line is a best fit of the slip model from eq. 8 obtaining an average slip length of $b = 318 \pm 44$ nm. On the right, we display a selection of 3 specific fields showing more distinct grouping with slip lengths b=0, 200 and 700 nm.

In Fig. 5 the endpoint k_r from Fig. 1 with $k_{r,o}(S_{cw})$>0.95 [1] are plotted versus r_e. For decreasing effective capillary radii r_e the relative permeabilities $k_{r,o}(S_{cw})$>1 increase to values as large as $k_{r,o}(S_{cw})$=14 . This trend qualitatively and quantitatively confirms the prediction by eq. 8: For a given slip length b the flux ratio or relative permeability is increasing when the pipe radius is decreasing. The solid line in Fig. 5 represents a best fit to the slip model from eq. 8 to both the aged and un-aged samples obtaining a slip length of b=318±44 nm displaying qualitative agreement with the experimental data.

Therefore the slip length b=318±44 μm is only an average and a possible range for the slip length is 0 nm≤b≤700 nm. This is well within the range of typical slip lengths reported in the literature. While the trend towards larger k_r endpoints for smaller pore diameters is clearly visible in the data, the data is not perfectly located on top of the fit line. The deviation of several data points from the fit line exceeds the (statistical) instrumental error. Either our large data set has systematic errors in k_r or in fact consists of several different populations that all have different slip lengths b. A subset of data for the individual fields groups more distinctly and follows more clearly the trend of the slip model. We find cases for no slip (b≈0 nm, field 1), intermediate slip (b≈200 nm, field 2) and maximum slip (b≈700 nm, field 3).

[1] for data without any measurement scatter the lower bound would have been set to 1 but we allowed for a 5 % error margin and therefore also included data points $k_{r,o}$>0.95 into the analysis

Often relative permeabilities with endpoints larger than 1 are "rescaled" by dividing both water and oil k_r by one common factor such that the largest endpoint is exactly 1.0. Using such a set of "rescaled" relative permeability curves for model predictions leads either to an under-prediction of the production rate or an over-prediction of the pressure drop, depending on the boundary conditions. In homogeneous rock the error arising from rescaling the relative permeability endpoints is lumped into other quantities like the absolute permeability. In a field development plan for an oil reservoir, pressure drop and/or flow rate are often constrained by independent parameters. Under-estimating the flow rate or over-estimating the pressure drop certainly has consequences during initial production. Although these errors might get detected in a history match, they may already have lead to a below-optimum production scenario in the field development plan. All these consequences are undesirable and therefore rescaling the k_r's should not be done.

5 CONCLUSIONS

Endpoint relative permeabilities $1 \le k_{r,o} \le 14$ have been observed experimentally in water-wet sandstone rock. A model employing capillary tubes with a *slip boundary condition* explains qualitatively and quantitatively the data with $k_r > 1$. The slip model predicts an increasing endpoint $k_{r,o}$ for a decreasing equivalent capillary radius r_e which is specifically confirmed by our data. On the microscopic scale, thin and presumably immobile wall coatings of the wetting phase are likely to cause the slip for the flow of the non-wetting phase. Thus slip seems to be related to wettability.

As the slip model provides a physical explanation for $k_r > 1$ consistent with findings in microfluidics and supported by the data in a specific way, there is no longer a basis for normalizing k_r endpoints to 1. Developers of pore network models are encouraged to extend their models with a slip boundary condition such that endpoint $k_r > 1$ would be possible to match experimental observations.

REFERENCES

ARPS&ROBERTS (1955) J. J. Arps, T. G. Roberts. *Trans. AIME*, 204:120, 1955.

AYUB&BENTSEN (1999) M. Ayub and R. G. Bentsen. *J. Petrol. Science and Engineering*, 23:13–29, 99.

BLAKE (1990) T. D. Blake. *Colloids Surf.*, 47:135, 1990.

BROCHARD ET AL. (1990) F. Brochard, P. G. DeGennes, S. M. Troian. *C. R. Acad. Sci.,* Ser II 310:1169, 1990.

BROCHARD&DEGENNES (1992) F. Brochard and P. G. de Gennes. *Langmuir*, 8:3033–3037, 1992.

CHOI ET AL. (2003) C.-H. Choi, K. J. A. Westin, S. Breuer. *Phys. Fluids*, 15(10):2897–2902, 2003.

CHOI&KIM (2006) C.-H. Choi and C.-J. Kim. *Phys. Rev. Lett*, 96:066001, 2006.

CHUAREV ET AL. (1984) N. V. Chuarev, V. D. Sobolev, A. N. Somov. *J. Coll. Interf. Sci.* 97, 574–581, 1984.

COTTIN-BIZONNE ET AL. (2005) C. Cottin-Bizonne, B. Cross, A. Steinberger, E. Charlaix. *Phys. Rev. Lett.*, 94: 056102, 2005.

DAKE (1978) L. P. Dake. *Fundamentals of Reservoir Engineering*. Elsevier B.V., 1978.

DEEN (1998) W. M. Deen. *Analysis of Transport Phenomena*. Oxford University Press, 1998.

DEGENNES (1985) P. G. de Gennes. *Review of Modern Physics*, 57(3):827–863, 1985.

DEGENNES (2002) P. G. de Gennes. *Langmuir*, 18:3413–3414, 2002.

DONG ET AL. (2006) M. Dong, F. A. L. Dullien, L. Dai, D. Li. *Transport on Porous Media* 63, 289–304, 2006.

DOSHI ET AL. (2005) D. A. Doshi, E. B. Watkins, J. N. Israelachvili, J. Majewski., *Proceedings of the National Academy of Sciences*, 102(27):9458–9462, 2005.

DULLIEN (1959) F. A. L. Dullien. *Porous Media - Fluid Transport and Pore Structure*. Academia Press, New York, 2nd ed. edition, 1992.

EHRLICH (1993) R. Ehrlich. *Transport in Porous Media*, 11:201–218, 1993.

HORN ET AL. (2000) R. Horn, O. Vinogradova, M. Mackay, N. Phan-Thien. *J. Chem. Phys.* 112, 6424–6433, 2000.

HUI&BLUNT (2000) M.-H. Hui, M. J. Blunt. Pore-scale modeling of three-phase flow and the effects of wettability. volume SPE 59309. Society of Petroleum Engineers, 2000.

KARABAKAL&BAGCI (2004) U. Karabakal, S. Bagci. *Energy & Fuels*, 18:438–449, 2004.

LAUGA&STONE (2003) E. Lauga, H. A. Stone. *Journal of Fluid Mech.*, 489, 55–77, 2003.

LORD&BUCKLEY (2002) D. L. Lord and J. S. Buckley. *Colloids and Surfaces A: Physicochem. Eng. Aspects*, 206:531–546, 2002.

MCPHEE (1994) C. A. McPhee. In *Advances in Petrophysics: 5 Years of Dialog*, pages 95–97. The London Petrophysical Society, July 1994.

MCPHEE&ARTHUR (1994) C. A. McPhee, K. G. Arthur. *SPE*, 28826:199–211, 1994.

MEZGER ET AL. (2006) M. Mezger, H. Reichert, S. Schöder, J. Okasinski, H. Schröder, H. Dosch, D. Palms, J. Ralston, V. Honkimäki. *PNAS*, 103:18401–18404, 2006.

MIGLER ET AL. (1993) K. B. Migler, H. Hervet, L. Leger. *Phys. Rev. Lett.*, 70, 286, 1993.

MIKKELSEN&SCHEIE (1991) M. Mikkelsen, A. Scheie. *SPE*, 22600:145–156, 1991.

MIKSIS&DAVIS (1994) S. H. Miksis, M. J. Davis. *Journal of Fluid Mech.*, 273:125–139, 1994

NAVIER (1827) C. L M. H. Navier. *Mem. Acad. Sci. Inst. Fr.*, 6:839, 1827.

ODEH (1959) A. S. Odeh, *Trans. AIME* 216, 346-353, 1959.

PRIEZJEV&TROIAN (2004) N. V. Priezjev and S. M. Troian. *Phys. Rev. Lett.*, 92(1):018302, 2004.

PRIEZJEV&TROIAN (2006) N.V. Priezjev and S.M. Troian. *J. Fluid Mech.*, 554:25, 2006.

RANSOHOFF&RADKE (1988) T. C. Ransohoff and C. J. Radke. *J. Colloid Interface Sci.*, 121(2):392–401, 1988.

SCHNELL (1956) E. Schnell. *J. Appl. Phys.*, 27:1149–1152, 1956.

THOMPSON&TROIAN (1997) P. A. Thompson, S. M. Troian. *Nature*, 389:360, 1997.

TOLSTOI (1952) D. M. Tolstoi. *Dokl. Acad. Nauk. SSSR*, 85:1089, 1952.

TRETHEWAY&MEINHART (2002) D. C. Tretheway and C. D. Meinhart. *Phys. Fluids*, 14(3):L9–L12, 2002.

TYRRELL&ATTARD (2001) J. W. G. Tyrrell, P. Attard. *Phys. Rev. Lett.* 87, 176104, 2001.

VINOGRADOVA (1995) O. I. Vinogradova. *Langmuir*, 11(6):2213, 1995.

VINOGRADOVA ET AL. (1995) O. I. Vinogradova, N. F. Bunkin, N. V. Chraev, O.A. Kiseleva, A. V. Lobeyev, and B. W. Ninham. *J. Colloid and Interface Sci.*, 173:443, 1995.

WATANABE ET AL. (1999) K. Watanabe, Y. Udagawa, H. Udagawa. *J. Fluid Mech.* 381, 225–238, 1999.

ZHU&GRANICK (2001) Y. Zhu and S. Granick. *Phys. Rev. Lett.*, 87:096105, 2001.

ZHU&GRANICK (2002) Y. Zhu and S. Granick. *Phys. Rev. Lett.*, 88:106102, 2002.